



# Bis-imidazolium-based anion-exchange membranes for alkaline fuel cells

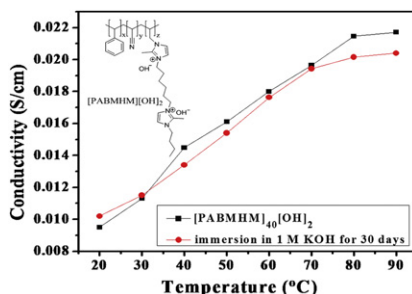
Bo Qiu<sup>1</sup>, Bencai Lin<sup>1</sup>, Zhihong Si, Lihua Qiu, Fuqiang Chu, Jie Zhao, Feng Yan\*

Jiangsu Key Laboratory of Advanced Functional Polymer Design and Application, Department of Polymer Science and Engineering, College of Chemistry, Chemical Engineering and Materials Science, Soochow University, Suzhou 215123, PR China

## HIGHLIGHTS

- ▶ We synthesize bis-imidazolium functionalized ionic liquid monomers.
- ▶ We prepare bis-imidazolium-based anion-exchange membranes.
- ▶ The membranes show a hydroxide conductivity up to  $2.0 \times 10^{-2} \text{ S cm}^{-1}$  at 60 °C.
- ▶ The membranes show an excellent chemical stability.

## GRAPHICAL ABSTRACT



## ARTICLE INFO

### Article history:

Received 12 April 2012

Received in revised form

8 June 2012

Accepted 9 June 2012

Available online 16 June 2012

### Keywords:

Anion exchange membrane

Bis-imidazolium-functionalized ionic liquids

Hydroxide conductivity

Chemical stability

## ABSTRACT

Novel anion-exchange membranes (AEMs) are prepared via in situ cross-linking of styrene, acrylonitrile and the bis-imidazolium functionalized ionic liquid monomer, 1-allyl-3-(6-(1-butyl-2-methylimidazol-3-ium-3-yl)hexyl)-2-methylimidazol-3-ium bromide ([ABMHM][Br]<sub>2</sub>), and followed by anion-exchange with hydroxide ions. The morphology and characteristic properties of the resultant copolymer membranes, such as the water uptake, swelling ratio, ion exchange capacity (IEC), hydroxide conductivity, and chemical stability are investigated. The membrane containing 40% mass fraction of [ABMHM][OH]<sub>2</sub> shows hydroxide conductivity up to  $2.0 \times 10^{-2} \text{ S cm}^{-1}$  and good long-term stability in 1 M KOH solution at 60 °C. The results of this study suggest that the AEMs based on bis-imidazolium cations have good perspectives for alkaline fuel cell applications.

© 2012 Elsevier B.V. All rights reserved.

## 1. Introduction

Fuel cells have been recognized as one of the most promising energy source systems that could provide clean and efficient energy for stationary and mobile applications [1–4]. The polymer electrolyte membrane, which acts as a separator between the fuel and oxidant streams and simultaneously transports ions is one of the very important components of a fuel cell [5–7]. The polymer

electrolyte membranes can be classified into two main types: proton-exchange membranes (PEMs) and anion-exchange membranes (AEMs), according to the charge carriers transported in the membranes. PEMs, represented by Nafion, exhibit excellent chemical, mechanical and thermal stability, as well as high proton conductivity when properly hydrated [5,8,9]. However, proton exchange membrane fuel cells (PEMFCs) are still facing challenges for commercialization due to high cost of the platinum catalysts, carbon monoxide poisoning of platinum catalysts at low temperature, and the limited working lifetime of PEMs [10,11]. Compared with PEMFCs, anion-exchange membrane fuel cells (AEMFCs) show enhanced oxygen reduction kinetics, extended choice of selective

\* Corresponding author. Tel.: +86 512 65880973; fax: +86 512 65880089.

E-mail address: [fyan@suda.edu.cn](mailto:fyan@suda.edu.cn) (F. Yan).

<sup>1</sup> Authors with equal contributions.

catalysts such as silver, cobalt or nickel. In addition, AEMFCs also offer the fuel flexibility, reduced fuel (such as methanol) crossover, and enhanced reaction kinetics for both oxygen reduction and fuel oxidation [12–14]. Therefore, there is growing interest in developing AEMs for AEMFCs application in recent years.

Various ionic polymers, such as polysulfone [15], poly(vinylbenzyl chloride- $\gamma$ -methacryloxypropyl trimethoxyl silane) [16], radiation-grafted poly(vinylidene fluoride) and poly(tetrafluoroethylene-co-hexafluoropropylene) [17–19] have been synthesized and used as AEMs for alkaline fuel cell applications. Most of these membranes were prepared via chloromethylation reaction and followed by quaternization using tertiary amines to form quaternary ammonium salts [2,5,9,15,20–22]. However, the long-term durability of the membranes in alkaline solution still need to be improved because hydroxide ions could degrade the quaternary ammonium cation sites on the polymeric AEMs via direct nucleophilic substitution or Hofmann elimination reaction, especially at high pH and elevated temperature [23]. Since the chemical stability of an AEM is strongly dependent on the nature of the cations, cations other than quaternary ammonium cation groups based polymers have been recently extensively studied. Compared with quaternary ammonium cations, however, quaternary phosphonium cations exhibited poorer alkine stability [24], and the conductivity of guanidinium cation based AEMs decreased quickly after be immersed in 0.5 M NaOH solution at 80 °C for 380 h [25].

Imidazolium type ionic liquids (ILs) are attracting wide attention because of their negligible vapor pressure, high ionic conductivity and excellent ion-exchange capability. Protic imidazolium type ILs have been successfully used in polymer electrolyte membrane fuel cells, which show high proton conductivity above 100 °C [10]. More recently, alkaline imidazolium functionalized AEMs have been synthesized and applied for alkaline fuel cell applications [3,8,12]. The membranes exhibit hydroxide ion conductivity above  $10^{-2}$  S cm $^{-1}$  at room temperature and show good alkaline stability probably due to the resonance effect of the conjugated imidazole rings, which weaken the interaction of

imidazolium groups and hydroxide ions. Although the stability of membranes still need to be improved [26–28], these results demonstrate a feasible approach for the synthesis and practical applications of alkaline imidazolium-type ILs functionalized AEMs, and should be expected to promote the widespread use of AEMFCs.

In this work, bis-imidazolium functionalized AEMs for alkaline fuel cells were synthesized. An IL monomer, 1-allyl-3-(6-(1-butyl-2-methylimidazol-3-ium-3-yl) hexyl)-2-methylimidazol-3-ium bromide ([ABMHM][Br] $_2$ ) was photocross-linked in situ with the proper monomer oils (styrene and acrylonitrile). The resulting membranes were converted to OH $^{-}$  form by changing the anions in the IL moiety of the copolymers with hydroxide anions, as shown in Scheme 1. The properties of the membranes, such as water uptake, swelling degree, ionic exchange capability (IEC), hydroxide ion conductivity, and chemical stability in high pH solution were investigated in details.

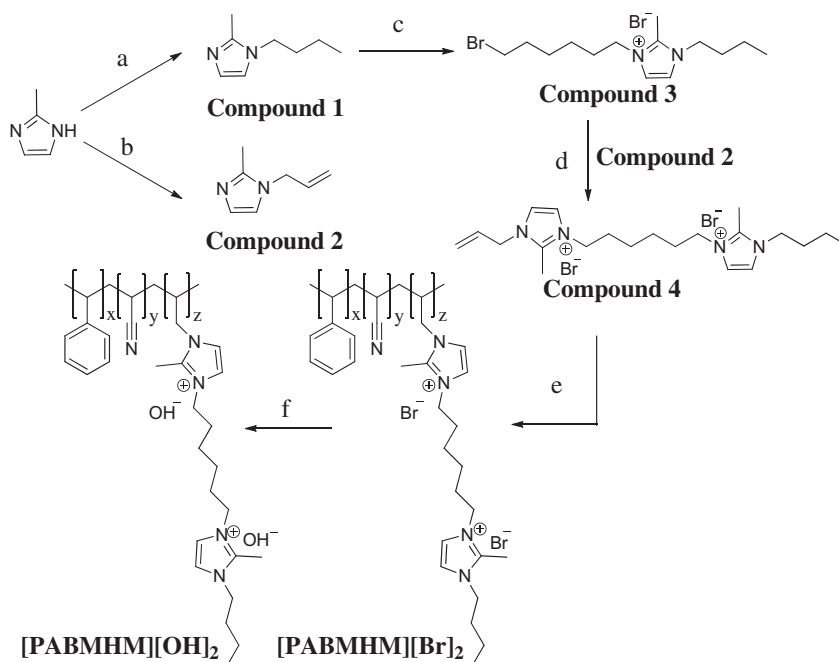
## 2. Experimental

### 2.1. Materials

Styrene, acrylonitrile, divinylbenzene (DVB), benzoin ethylether, ethylether, ethanol, 2-methylimidazole, 1-bromobutane, methanol, allyl bromide, 1, 6-dibromohexane, phenolphthalein, potassium hydroxide, acetonitrile, acetone, methylene dichloride, ethyl acetate, sodium hydroxide, hydroquinone, and hydrochloric acid were used as purchased. All of vinyl monomers were made inhibitor-free by passing the liquid through a column filled with neutral Al $_2$ O $_3$ . Distilled deionized water was used for all experiments.

### 2.2. Synthesis of 1-butyl-2-methylimidazole (Compound 1) and 1-allyl-2-methylimidazole (Compound 2)

1-Butyl-2-methylimidazole was synthesized in acetonitrile (50 ml) by stirring the mixture of 2-methylimidazole (3 g), 1-bromobutane (5 g) and NaOH (4.09 g) at room temperature for



**Scheme 1.** Synthetic procedure for the anion-exchange membranes. (a) 1-bromobutane, NaOH, room temperature, 4 h; (b) allyl bromide, NaOH, room temperature, 4 h; (c) 1, 6-dibromohexane, 50 °C, 2 days, (d) hydroquinone, 50 °C, 2 days, (e) styrene, acrylonitrile, DVB, photo-cross linking, 0.5 h, (f) 1 M KOH solution, 60 °C, 24 h.

4 h. After filtrating, the filtrate was dissolved in deionized water, followed by extraction using methylene dichloride. The mixture was evaporated at 30 °C to yield the product.  $^1\text{H}$  NMR (400 MHz,  $\text{CDCl}_3$ ): 6.88 (1H, s), 6.79 (1H, s), 3.80 (2H, t), 2.36 (3H, s), 1.68 (2H, m), 1.33 (2H, m), 0.92 (3H, t).

1-Allyl-2-methylimidazole was synthesized follow the method as described above: A mixture of 2-methylimidazole (3.39 g), allyl bromide (5 g) and NaOH (4.63 g) was stirred at room temperature for 4 h and then filtrated.  $^1\text{H}$  NMR (400 MHz,  $\text{CDCl}_3$ ): 6.91 (1H, s), 6.79 (1H, s), 5.90 (1H, m), 5.20 (1H, d), 4.98 (1H, d), 4.45 (2H, s), 2.34 (3H, s).

### 2.3. Synthesis of 3-(6-bromohexyl)-1-butyl-2-methylimidazol-3-ium bromide ([BHBMMI][Br]) (Compound 3)

[BHBMMI][Br] was synthesized by stirring a mixture containing 1-butyl-2-methylimidazole and 1, 6-dibromohexane (molar ratio = 1:3) in 50 ml ethanol at 50 °C for two days. After the evaporation of solvent, the resultant viscous oil was wash with ethyl acetate and ethylether three times, respectively. The solvent was removed and the residue was purified by silica gel column chromatography using methanol/acetone 1/3 (v/v) as the eluent to obtain viscous liquid.  $^1\text{H}$  NMR (400 MHz,  $\text{D}_2\text{O}$ ): 7.32 (2H, s), 4.06 (4H, m), 3.44 (2H, t), 2.55 (3H, s), 1.80 (6H, m), 1.40 (2H, m), 1.30 (4H, m), 0.87 (3H, t).

### 2.4. Synthesis of 1-allyl-3-(6-(1-butyl-2-methylimidazol-3-ium-3-yl)hexyl)-2-methylimidazol-3-ium bromide ([ABMHM][Br]<sub>2</sub>) (Compound 4)

[ABMHM][Br]<sub>2</sub> was synthesized by stirring a mixture containing 1-allyl-2-methylimidazole and [BHBMMI][Br] (molar ratio = 1.5:1) in 50 ml ethanol at 50 °C for two days. After the evaporation of solvent, the resultant viscous oil was wash with ethyl acetate and ethylether three times, respectively. The solvent was removed and the residue was purified by silica gel column chromatography using methanol/acetone 1/3 (v/v) as the eluent to obtain viscous liquid.  $^1\text{H}$  NMR (400 MHz,  $\text{D}_2\text{O}$ ): 7.31 (2H, s), 7.08 (1H, d), 6.98 (1H, d), 5.95 (1H, m), 5.20 (1H, d), 4.94 (1H, d), 4.55 (2H, d), 4.05 (4H, m), 3.43 (2H, t), 2.54 (3H, s), 2.34 (3H, s), 1.75 (6H, m), 1.40 (2H, m), 1.25 (4H, m), 0.85 (3H, t).

### 2.5. Preparation of anion exchange membranes

The AEMs were synthesized as follows: a mixture of styrene/acrylonitrile (1:3 weight ratio), [ABMHM][Br]<sub>2</sub>, divinylbenzene (4 wt%, based on the weight of monomer), and 2 wt% of benzoin ethylether (as a photoinitiator) was stirred and ultrasonicated to obtain a homogeneous solution, which was then cast into a glass mold and photo-cross-linked via irradiation with ultraviolet (UV) light (wavelength of 250 nm) in a glass mold for 30 min at room temperature. Then it was immersed in  $\text{N}_2$ -saturated 1 M KOH solution at 60 °C for 24 h to convert the membrane from  $\text{Br}^-$  to  $\text{OH}^-$  form. This process was repeated three times to ensure complete conversion. Then the converted membranes were immersed in  $\text{N}_2$ -saturated deionized water for 24 h and washed with deionized water until the pH of residual water was neutral.

### 2.6. Characterization

$^1\text{H}$  NMR spectra were recorded on a Varian 400 MHz spectrometer. Fourier transform infrared (FT-IR) spectra of the membranes were recorded on a Varian CP-3800 spectrometer in the range of 4000–400  $\text{cm}^{-1}$ . Thermal analysis was carried out by Universal Analysis 2000 thermogravimetric analyzer (TGA).

Samples were heated from 70 to 500 °C at a heating rate of 15 °C  $\text{min}^{-1}$  under a nitrogen flow. The tensile properties of the membranes were measured by using an Instron 3365 at 25 °C at a crosshead speed of 5 mm  $\text{min}^{-1}$ . Scanning electron microscopy (SEM) images were taken with a Philips Model XL 30 FEG microscope with an accelerating voltage of 10 kV. Energy-dispersive X-ray spectroscopy (EDX) measurements were performed with the spectrometer attached on the Hitachi Model S-4700 field-emission scanning electron microscopy (SEM) system.

### 2.7. Liquid uptake and swelling ratio

The dried membrane samples were weighed ( $W_d$ ) and immersed in  $\text{N}_2$ -saturated distilled water or methanol at room temperature for 24 h. Then the hydrated polymer membranes were taken out, and the excess water or methanol on the surface was removed by wiping with a tissue paper and weighed immediately ( $W_w$ ). The water (or methanol) uptake  $W$  was calculated with the following equation:

$$W(\%) = \frac{(W_w - W_d)}{W_d} \times 100\%$$

The swelling ratio was characterized by linear expansion ratio (LER), which was determined by the difference between wet and dry dimensions of a membrane sample (4 cm in length and 2 cm in width). The calculation was based on the following equation:

$$\text{Swelling}(\%) = \frac{X_{\text{wet}} - X_{\text{dry}}}{X_{\text{dry}}} \times 100\%$$

where  $X_{\text{wet}}$  and  $X_{\text{dry}}$  are the lengths of wet (in water or methanol) and dry membranes, respectively.

### 2.8. Liquid uptake and swelling ratio

Ion exchange capacity (IEC) was determined via a back-titration. The membranes were dried and weighed before immersing into 100 ml of 0.01 M HCl standard solution for 48 h. The solutions were then titrated with a standardized NaOH solution using phenolphthalein as an indicator. The IEC value was calculated as follows:

$$\text{IEC} = \frac{V_{0,\text{NaOH}}C_{\text{NaOH}} - V_{x,\text{NaOH}}C_{\text{NaOH}}}{m_{\text{dry}}}$$

where  $V_{0,\text{NaOH}}$  and  $V_{x,\text{NaOH}}$  are the volume of the NaOH consumed in the titration without and with membranes, respectively,  $C_{\text{NaOH}}$  is the molar concentration of the NaOH, which is titrated by the standard oxalic acid solution, and  $m_{\text{dry}}$  is the mass of the dry membranes. Each sample was replicated for three times.

### 2.9. Hydroxide ion conductivity

The ionic conductivity was measured by two-point probe AC impedance spectroscopy with the electrochemical equipment (CHI660C) rather than the four probe one [5,29,30] which is thought to have overestimated the ionic conductivity, with the frequency range from 1 Hz to 100 kHz. All the samples were fully hydrated in  $\text{N}_2$ -saturated deionized water for at least 24 h prior to the conductivity measurement. To maintain the relative humidity at 100% during the experiments, conductivity measurements were conducted in a chamber filled with  $\text{N}_2$ -saturated deionized water under fully hydrated conditions. The ionic conductivity of the membrane,  $\sigma$  ( $\text{S cm}^{-1}$ ), can be calculated from the equation:



Fig. 1. Photographs of [PABMHM]<sub>40</sub>[OH]<sub>2</sub> with a thickness of 45 μm.

$$\sigma = \frac{l}{RA}$$

where  $l$  is the distance between two gold electrodes (given in centimeters (cm)),  $A$  is the cross-sectional area of membrane (cm<sup>2</sup>) and  $R$  is the membrane resistance value from the AC impedance data ( $\Omega$ ).

### 3. Results and discussion

#### 3.1. Preparation of anion exchange membranes

The crosslinked AEMs were prepared via in situ photo-cross linking of a mixture containing [ABMHM][Br]<sub>2</sub> (30–40 wt.%), styrene/acrylonitrile (1:3 weight ratio, 70–60 wt.%), and DVB (4 wt.% based on the weight of monomer) in a glass mold, followed by ion exchange with OH<sup>−</sup> (Scheme 1). The resultant copolymers were denoted as [PABMHM]<sub>x</sub>[OH]<sub>2</sub> (the subscript  $x$  indicates the weight ratio of [ABMHM][OH]<sub>2</sub>). As shown in Fig. 1 that the prepared [PABMHM]<sub>30</sub>[OH]<sub>2</sub>, [PABMHM]<sub>40</sub>[OH]<sub>2</sub> are transparent, flexible, and can be easily cut into any desired sizes. The SEM images show that the resultant membranes in OH<sup>−</sup> form are uniform, compact, smooth and without any visible pores on the surface and in the interior of the membranes (Fig. 2A and B).

#### 3.2. FT-IR spectra and energy-dispersive X-ray (EDX) spectra

Fig. 3 shows the Fourier transform infrared (FT-IR) spectra of the membranes in Br<sup>−</sup> and OH<sup>−</sup> forms. Membranes in both two forms

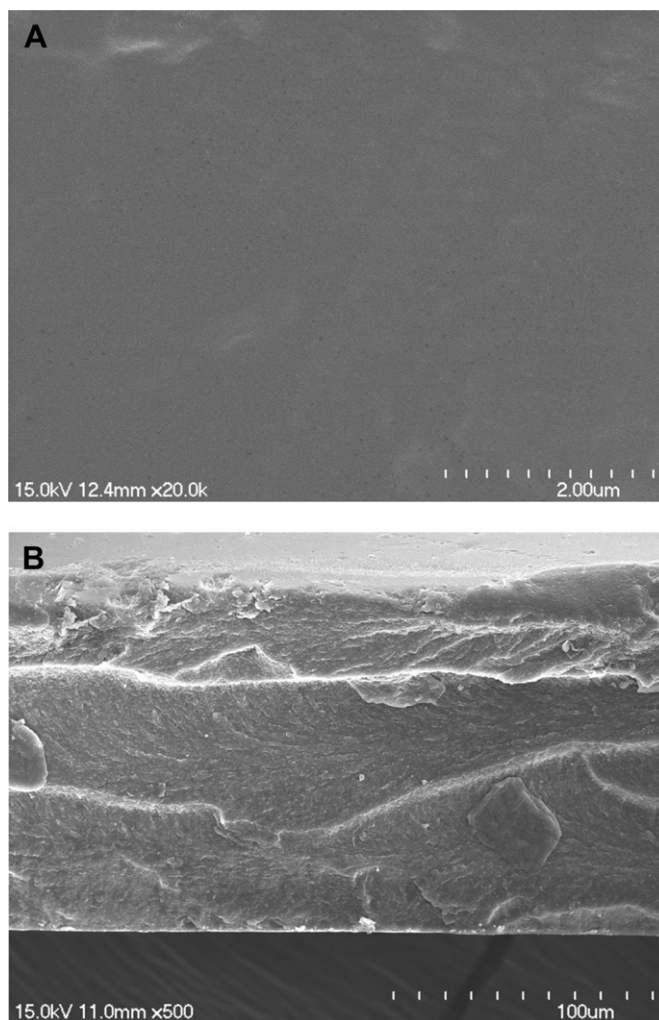


Fig. 2. SEM images of the [PABMHM]<sub>40</sub>[OH]<sub>2</sub> (thickness of 150 μm): (A) surface view and (B) cross-sectional view of [PABMHM]<sub>40</sub>[OH]<sub>2</sub> membranes.

show the absorption bands of the cyano groups (C≡N) at 2235 cm<sup>−1</sup>. The peaks at 3030–3063 and 1450–1600 cm<sup>−1</sup> confirm the existence of polystyrene. Absorption peaks at 766 cm<sup>−1</sup> arise from the vibrational mode of imidazolium cations. A wide absorption peak at 3300–3600 cm<sup>−1</sup> in the OH<sup>−</sup> form membranes (Fig. 3B) is attributed to the stretching vibration of O–H groups, indicating the successful anion change from Br<sup>−</sup> form to OH<sup>−</sup> form. Furthermore, the results of energy-dispersive X-ray (EDX) spectra

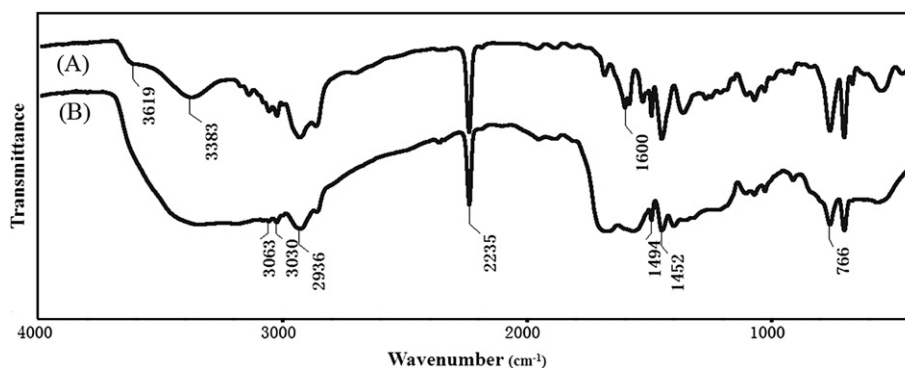


Fig. 3. FT-IR spectra of (A) [PABMHM]<sub>40</sub>[Br]<sub>2</sub> and (B) [PABMHM]<sub>40</sub>[OH]<sub>2</sub>.



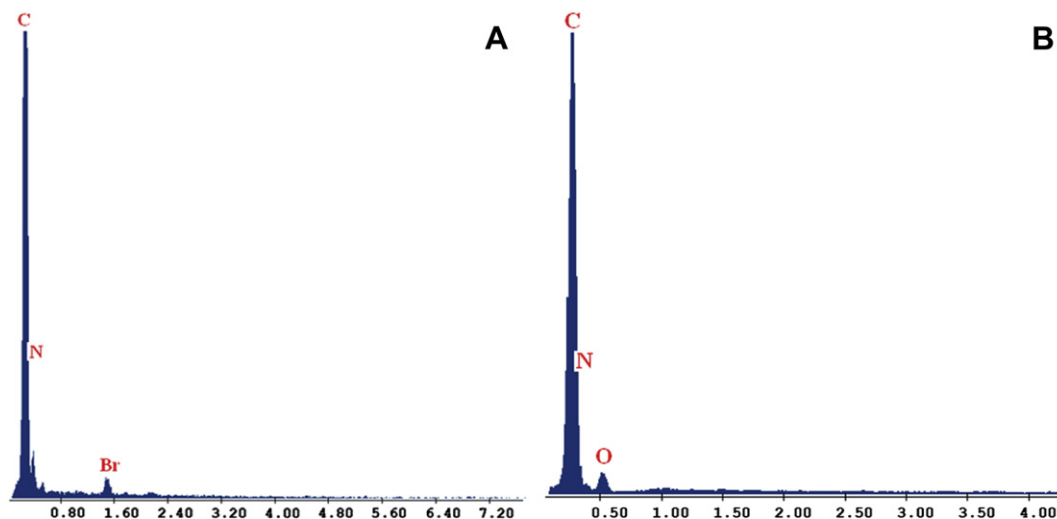


Fig. 4. Energy-dispersive X-ray (EDX) spectra for (A) [PABMHM]<sub>40</sub>[Br]<sub>2</sub> and (B) [PABMHM]<sub>40</sub>[OH]<sub>2</sub>.

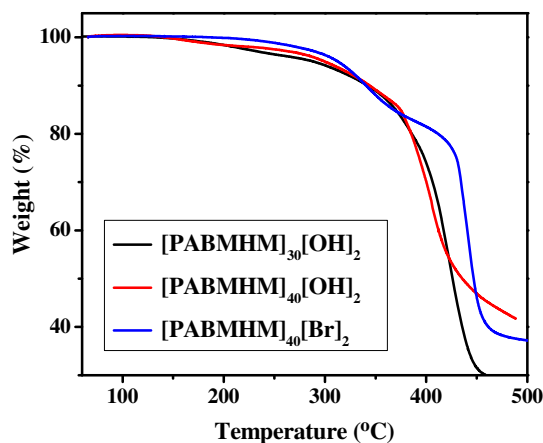


Fig. 5. Thermogravimetric analyzer (TGA) curves of membranes under nitrogen flow, heating rate: 15 °C min<sup>−1</sup>.

show that no Br<sup>−</sup> or K<sup>+</sup> ions could be detected in the OH<sup>−</sup> form (Fig. 4B), which further confirm the successful anion change of membranes.

### 3.3. Thermal analysis

Fig. 5 shows the typical thermogravimetric analyzer (TGA) curves of produced AEMs in Br<sup>−</sup> and OH<sup>−</sup> forms, which were recorded under a nitrogen flow from 70 to 500 °C at a heating rate of 15 °C min<sup>−1</sup> to assess their thermal stabilities. Membranes in both two forms show good thermal stability. The weight loss region at temperatures above 300 °C may due to the degradation of the copolymer backbone and imidazolium side chain. Polymers based on the aromatic backbones, such as poly(arylene ether sulfone)s and poly(arylene ether ketone)s, are generally considered as the preferred candidates for high-temperature fuel-cell applications

because of their excellent thermal stability. Here, we can see that the thermal stability of the bis-imidazolium-based AEMs is comparable to that of quaternary ammonia polysulfone [9] and quaternary guanidinium poly(arylene ether sulfone)s containing hydroxide groups [31,32].

### 3.4. Ion exchange capacity (IEC), water (methanol) uptake and swelling ratio and mechanical properties

IEC of the membranes reflects the exchangeable groups in the membranes. Water uptake and swelling behavior of the membranes are essential factors influencing the morphologic stability of membranes. Table 1 shows the values of IEC, water/methanol uptake, and swelling degree of the produced AEMs. The experimental IEC value of [PABMHM]<sub>x</sub>[OH]<sub>2</sub> is close to the theoretical value, which increased with the content of IL, accompanied with higher water/methanol uptake and swelling degree. We assume that the high content of OH<sup>−</sup> ions leads to the formation of the larger ion clusters within the membrane and thus led to the absorption of more water [33]. Both of the prepared AEMs display lower swelling degree in pure methanol than that in water, also lower than that of Nafion-117 in methanol (34.50%) under the same experimental conditions. These results are might due to the different adsorption capacity between liquid molecules and copolymers. The membrane absorbs water more easily than methanol [34]. Since the use of more-concentrated fuels leads to higher energy densities, it suggests a feasible approach for practical applications in direct methanol fuel cells. The tensile strength and the Young's modulus decrease when the membranes were saturated with water and methanol. It can be seen that the [PABMHM]<sub>40</sub>[OH]<sub>2</sub> membrane shows the tensile strength of 25.10 MPa, a Young's modulus of 1160.29 MPa, and an elongation at break of 12.61% (Table 2). Compared with the [PABMHM]<sub>40</sub>[OH]<sub>2</sub> membranes, both the tensile strength and Young's modulus of

**Table 1**  
The values of water (methanol) uptakes, swelling degree and IEC for the [PABMHM]<sub>x</sub>[OH]<sub>2</sub>.

Sample	IEC(m equiv g <sup>−1</sup> )		Water uptake (%)	Swelling degree in water (%)	Methanol uptake (%)	Swelling degree in methanol (%)
	Theoretical	Experimental				
[PABMHM] <sub>30</sub> [OH] <sub>2</sub>	1.122	0.998	40.50	11.86	5.15	2.30
[PABMHM] <sub>40</sub> [OH] <sub>2</sub>	1.496	1.416	65.36	13.58	5.59	3.70
Nafion-117 [3]	—	—	19.48	6.09	47.58	34.50

**Table 2**  
Mechanical properties of [PABMHM]<sub>40</sub>[OH]<sub>2</sub>.

Membrane	Tensile strength (MPa)	Tensile modulus (MPa)	Elongation at break (%)
[PABMHM] <sub>40</sub> [OH] <sub>2</sub>	25.10	1160.29	12.61
[PABMHM] <sub>40</sub> [OH] <sub>2</sub> saturated with water	19.50	890.34	16.42
[PABMHM] <sub>40</sub> [OH] <sub>2</sub> saturated with methanol	24.30	1056.89	13.35

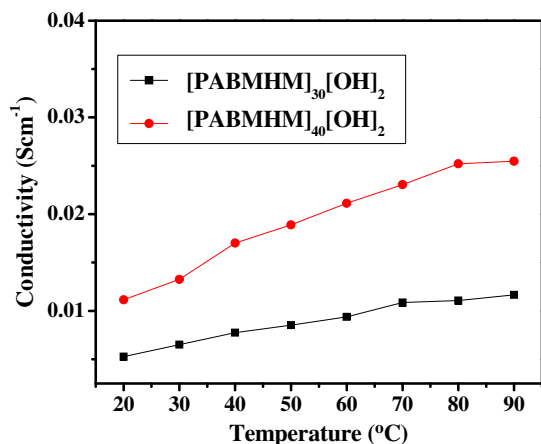


**Fig. 6.** Variations in ionic conductivities of [PABMHM]<sub>x</sub>[OH]<sub>2</sub> as a function of temperature.

water- and methanol-saturated membranes slightly decreased, while the elongation at break value was enhanced due to the plasticizing effect of the solvent. These results indicate that the AEMs prepared in this work are tough and ductile enough for the potential use as AEM materials.

### 3.5. Ionic conductivity and chemical stability

The ionic conductivity of the OH<sup>−</sup> form membrane as a function of the temperature is shown in Fig. 6. The conductivity of the membranes increases with the temperature increasing because the free volume in favor of ion transport and the mobility of anions is increased as the temperature rises. [PABMHM]<sub>40</sub>[OH]<sub>2</sub> shows the highest conductivity up to  $2.5 \times 10^{-2}$  S cm<sup>−1</sup> at 90 °C, fulfills the basic conductivity requirement of fuel cells, which is 2.5 times higher than that of [PABMHM]<sub>30</sub>[OH]<sub>2</sub> at the same temperature.

From the view point of applications, AEMs should be stable in alkaline solution, especially at high pH and elevated temperature.

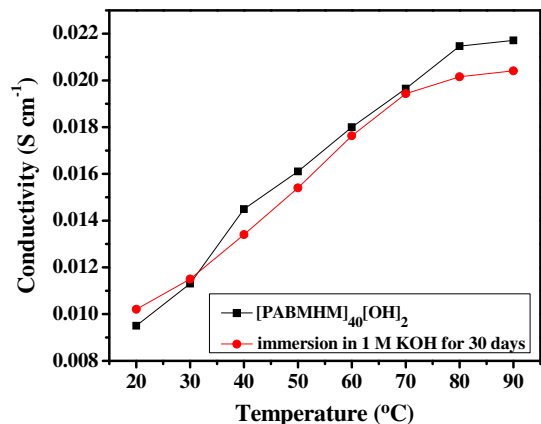


**Fig. 7.** Variations in ionic conductivities of [PABMHM]<sub>40</sub>[OH]<sub>2</sub> before and after immersion in 1 M KOH at 60 °C for 30 days as a function of temperature.

**Table 3**  
The ion exchange capacity (IEC) values of [PABMHM]<sub>40</sub>[OH]<sub>2</sub> membranes be immersed in 1 M KOH solution at 60 °C.

Time immersed in 1 M KOH (h)	IEC (m equiv g <sup>−1</sup> )
24	1.416 ± 0.045
48	1.400 ± 0.055
72	1.435 ± 0.040
96	1.383 ± 0.085
120	1.395 ± 0.050

Here, the alkaline stability of [PABMHM]<sub>40</sub>[OH]<sub>2</sub> was investigated by immersing the samples into 1 M KOH solution at 60 °C to check the changes of ionic conductivity. Fig. 7 shows the hydroxide conductivity of [PABMHM]<sub>40</sub>[OH]<sub>2</sub> before and after treatment with 1 M KOH at 60 °C for 30 days. No obvious decrease of the conductivity could be observed, indicating an good chemical stability of [PABMHM]<sub>40</sub>[OH]<sub>2</sub> membrane in KOH solution. The IEC value of [PABMHM]<sub>40</sub>[OH]<sub>2</sub> membranes showed slight fluctuations during the stability test, which further confirms the good alkaline stability of the membranes (Table 3). The good alkaline stability of [PABMHM]<sub>40</sub>[OH]<sub>2</sub> is probably due to the resonance effect of the conjugated imidazole rings, which reduce the positive charge density of the cation and weaken the interaction with the hydroxide ions, and thus dramatically improve the imidazolium-functionalized AEMs [27,34].

## 4. Conclusions

In summary, novel AEMs based on bis-imidazolium-functionalized ionic liquid monomer were prepared via in situ photo-cross-linking and followed by anion exchange with OH<sup>−</sup>. The resultant membranes are flexible and tough enough for potential use as AEMs for AEMFC applications. The thin films contained [ABMHM][OH]<sub>2</sub> with a mass fraction of 40 wt% exhibit hydroxide conductivity above  $10^{-2}$  S cm<sup>−1</sup> at room temperature and the good chemical stability in high pH solution at 60 °C, indicating that the membranes could overcome the alkaline instability of the alkyl quaternary ammonium functionalized polymers and fulfill the basic require of AEMFCs.

## Acknowledgments

This work was supported by Natural Science Foundation of China (Nos. 20974072, 21174102), The Natural Science Foundation of Jiangsu Province (BK2011274), Program for Scientific Innovation Research of College Graduate in Jiangsu Province (CXZZ11-0103) and the Project Funded by the Priority Academic Program Development of Jiangsu Higher Education Institutions.

## References

- [1] B.C.H. Steele, A. Heinzel, Nature 414 (2001) 345–352.
- [2] M. Tanaka, K. Fukasawa, E. Nishino, S. Yamaguchi, K. Yamada, H. Tanaka, B. Bae, K. Miyatake, M. Watanabe, J. Am. Chem. Soc. 133 (2011) 10646–10654.
- [3] B. Lin, L. Qiu, B. Qiu, Y. Peng, F. Yan, Macromolecules 44 (2011) 9642–9649.
- [4] K. Matsumoto, T. Fujigaya, H. Yanagi, N. Nakashima, Adv. Funct. Mater. 21 (2011) 1089–1094.
- [5] T.J. Clark, N.J. Robertson, H.A. Kostalik IV, E.B. Lobkovsky, P.F. Mutolo, H.D. Abruna, G.W. Coates, J. Am. Chem. Soc. 131 (2009) 12888–12889.
- [6] A.J. Appleby, R.L. Foulkes, Fuel Cell Handbook, Van Nostrand Reinhold, New York, 1989.
- [7] M.S. Whittingham, R.F. Savinelli, T.A. Zawodzinski, Chem. Rev. 104 (2004) 4243–4244.
- [8] B. Qiu, B. Lin, L. Qiu, F. Yan, J. Mater. Chem. 22 (2012) 1040–1045.
- [9] J. Pan, S. Lu, Y. Li, A. Huang, L. Zhuang, J. Lu, Adv. Funct. Mater. 20 (2010) 312–319.
- [10] B. Lin, L. Qiu, J. Lu, F. Yan, Chem. Mater. 22 (2010) 1807–1813.
- [11] S. Lu, J. Pan, A. Huang, L. Zhuang, J. Lu, Proc. Natl. Acad. Sci. U. S. A. 105 (2008) 20611–20614.

- [12] B. Lin, L. Qiu, J. Lu, F. Yan, *Chem. Mater.* 22 (2010) 6718–6725.
- [13] E. Antolini, E.R. Gonzalez, *J. Power Sources* 195 (2010) 3431–3450.
- [14] J.A. Vega, C. Chartier, W.E. Mustain, *J. Power Sources* 195 (2010) 7176–7180.
- [15] M.R. Hibbs, M.A. Hickner, T.M. Alam, S.K. McIntyre, C.H. Fujimoto, C.J. Cornelius, *Chem. Mater.* 20 (2008) 2566–2573.
- [16] C. Wu, Y. Wu, J. Luo, T. Xu, Y. Fu, *J. Membr. Sci.* 356 (2010) 96–104.
- [17] T.N. Danks, R.C.T. Slade, J.R. Varcoe, *J. Mater. Chem.* 13 (2003) 712–721.
- [18] T.N. Danks, R.C.T. Slade, J.R. Varcoe, *J. Mater. Chem.* 12 (2002) 3371–3373.
- [19] R.C.T. Slade, J.R. Varcoe, *Solid State Ionics* 176 (2005) 585–597.
- [20] J.R. Varcoe, R.C.T. Slade, *Fuel Cells* 5 (2005) 187–200.
- [21] G. Couture, A. Alaaeddine, F. Boschet, B. Ameduri, *Prog. Polym. Sci.* 36 (2011) 1521–1557.
- [22] Y. Wan, B. Peppley, K.A.M. Creber, V. Tam Buia, *J. Power Sources* 195 (2009) 3785–3793.
- [23] H. Hou, G. Sun, R. He, B. Sun, W. Jin, H. Liu, Q. Xin, *Int. J. Hydrogen Energy* 33 (2008) 7172–7176.
- [24] S. Gu, R. Cai, T. Luo, K. Jensen, C. Contreras, Y. Yan, *ChemSusChem* 3 (2010) 555–558.
- [25] D. Kim, A. Labouriau, M.D. Guiver, Y. Kim, *Chem. Mater.* 23 (2011) 3795–3797.
- [26] Y. Ye, Y.A. Elabd, *Macromolecules* 44 (2011) 8494–8503.
- [27] F. Zhang, H. Zhang, C. Qu, *J. Mater. Chem.* 21 (2011) 12744–12752.
- [28] J. Ran, L. Wu, J.R. Varcoe, A.L. Ong, S.D. Poynton, T. Xu, *J. Membr. Sci.*, <http://dx.doi.org/10.1016/j.memsci.2012.05.006>.
- [29] N.J. Robertson, H.A. Kostalik IV, T.J. Clark, P.F. Mutolo, H.D. Abruna, G.W. Coates, *J. Am. Chem. Soc.* 132 (2010) 3400–3404.
- [30] J. Pan, C. Chen, L. Zhuang, J. Lu, *Acc. Chem. Res.* 45 (3) (2012) 473–481.
- [31] J. Wang, S. Li, S. Zhang, *Macromolecules* 43 (2010) 3890–3896.
- [32] J. Wang, Z. Zhao, F. Gong, S. Li, S. Zhang, *Macromolecules* 42 (2009) 8711–8717.
- [33] C.H. Lee, H.B. Park, Y.S. Chung, Y.M. Lee, B.D. Freeman, *Macromolecules* 39 (2006) 755–764.
- [34] M. Guo, J. Fang, H. Xu, W. Li, X. Lu, C. Lan, K. Li, *J. Membr. Sci.* 362 (2010) 97–104.